Finite element analysis of fretting contact for nonhomogenous materials

IOP Conf. Series: Materials Science and Engineering **295** (2018) 012006 doi:10.1088/1757-899X/295/1/012006

Finite element analysis of fretting contact for nonhomogenous materials

***Korkmaz Y M*[1,2], *Coker D*[1]**
[1]*Middle East Technical University, Department of Aerospace Engineering, 06800, Ankara, Turkey*
[2]*Helicopter group, Turkish Aerospace Industries, 06800, Ankara, Turkey*
yedzdanmedet.korkmaz@tai.com.tr[1], *coker@metu.edu.tr*[2]

Abstract: *Fretting problem arises in the case of relatively small sliding motion between contacting surfaces. Fatigue life of the components that are in contact with each other, especially in rotorcraft may be significantly reduced due to fretting. The purpose of this study is to investigate material inhomogeneity near the contact region on the fretting problem in a cylindrical on flat contact configuration. A finite element (FE) model was constructed by using commercial finite element package ABAQUS™to study partial sliding and stress concentrations. In order to investigate the effect of material inhomogeneity, the fretting contact is analyzed by introducing voids near the contact region. The void size and an array of voids is introduced into the substrate. The results are compared in terms of pressure, shear traction, tangential stress magnitudes and relative slip between the contacting materials.*

Keywords: fretting; finite element modelling; contact modelling

1. Introduction

When relative small sliding takes in place between two contacting surfaces, failure due to fretting can occur, such as bolted joints and lug attachments of aircrafts. Waterhouse [1] mentioned that bolted and riveted structures which are subjected to fluctuating loads are possible sources of fretting fatigue failures in his works. In order to investigate the fretting phenomena, there are numerous studies which were done with using both analytical and finite element (FE) methods can be found in literature. To observe the pressure distribution in the frictionless contact region between two elastic materials, the analytical approach is developed by Hertz [2] which is called Hertzian contact theory. Later, to observe the effect of the both tangential loading and corresponding friction at the contact interface Mindlin and Deresiewicz [3] further improved Hertz contact theory. Mindlin theory divides the contact interface in two main regions, which are called as stick and slip, with using shear traction distribution. Furthermore, the effect of the bulk stress in calculations of the shear traction distribution taken in consideration by Hills and Nowell [4]. In addition to that Nowell [5] reported that Mindlin theory is inadequate to calculate shear traction distribution for contact between elastically dissimilar materials. Finite element analysis provides has an opportunity to discover and simulate different contact conditions by taking the geometrical non-linearity into account for various geometries. Numerous works were done in the literature in order to model fretting contact by using finite element methods. For instance, Ruiz et al. [6] and Stower et al. [7] simulated fretting contact using FEA. The

effect of dissimilar materials on fretting fatigue behavior of Ti-6Al-4V was shown by Lee and Mall [8]. Simulation of the crack propagation were performed in the contact region with using extended finite element method by Giner et al. [9]. The differences between 2D and 3D finite element analysis of the fretting fatigue were investigated Kim et al. [10]. Korkmaz and Coker [11] simulated the contact and friction behavior of dissimilar materials using finite element method. In this study, we investigate the effect of material inhomogeneity in cylindrical on flat fretting contact configuration by introduction of voids in the substrate near the contact region.

2. Theoretical Background

Hertzian contact theory is used to calculate the contact pressure and to determine the contact area between the two different elastic bodies without friction (Figure 1). This theory is only applicable when the effective radius of curvature is much greater than the semi contact width. In accordance with Hertzian theory, the contact pressure becomes maximum at the center of the contact region and

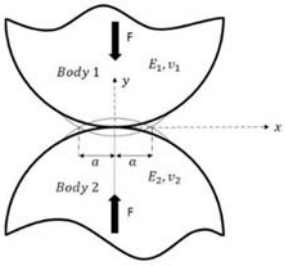

Figure 1. Representative view of Hertzian contact.

becomes zero at the edges when two cylindrical bodies are in contact,

$$p(x) = -\frac{2F}{\pi a l}\sqrt{a^2 - x^2} \tag{1}$$

where $p(x)$ is the contact pressure, F is the normal load, l is the thickness, and a is the contact radius given by,

$$a = \sqrt{\frac{2F}{\pi}\left(\frac{1-v_1^2}{E_1} + \frac{1-v_2^2}{E_2}\right)\left(\frac{1}{R_1} + \frac{1}{R_2}\right)} \tag{2}$$

where E_i, v_i, R_i are the elastic modulus, Poisson's ratio and radius of the top and bottom surfaces for $i=1,2$.

The contact region is divided into two regions consisting of stick and slip regions (Figure 2). Part of the contact region where there is no relative displacement between the pad and the specimen is called the stick region and the other part where there is relative displacement is called the slip region [12].

The shear traction distribution, $q(x)$, is calculated by,

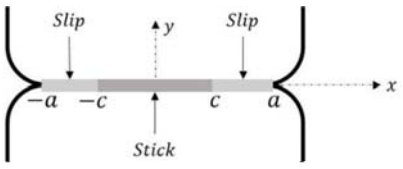

Figure 2. Representative view of the stick slip relation in the contact region.

$$q(x)=\begin{cases} -fp_{\max}\sqrt{1-(x/a)^2} & c\le|x|\le a \\ -fp_{\max}\left[\sqrt{1-(x/a)^2}-2\dfrac{c}{a}\sqrt{1-(x/c)^2}\right] & |x|<c \end{cases} \tag{3}$$

Where f is the friction coefficient and c is the length of the stick region given by,

$$\frac{c}{a}=\sqrt{1-\frac{Q}{2fF}} \tag{4}$$

However, when the shear loading is generated by an axial bulk stress applied to one component, the stick region is shifted by the eccentricity value e which causes a change in the shear traction distribution given by the following equation,

$$q(x)=\begin{cases} -fp_{\max}\sqrt{1-(x/a)^2} & c\le|x|\le a \\ -fp_{\max}\left[\sqrt{1-(x/a)^2}-2\dfrac{c}{a}\sqrt{1-\left(\dfrac{x+e}{c}\right)^2}\right] & |x+e|<c \end{cases} \tag{5}$$

3. Finite element modelling

Finite element model of a cylinder on flat contact configuration is simulated with ABAQUS™. Half of the specimen is modelled due to symmetry conditions in the y-direction and the vertical movement along the bottom symmetry axis is restricted. A specimen with length *L=40 mm*, width *w=5mm* and thickness *t*=4mm was used [13]. The radius of the pad, *R*, was chosen as 10mm. In FE model, where a uniform axial stress is applied to the right boundary, the cylinder pad is restricted in the horizontal direction along its side surfaces and is free to move in the vertical direction (Figure 3). The loading is applied to the model in two steps. In the first step, normal load is applied. In step 2 axial stress and a reaction is applied while keeping the normal stress constant as shown in Table 1.

Table 1. The loading conditions of fretting fatigue contact [14].

	Step 1	Step 2
Normal Load [N]	543	543
Axial stress [MPa]	0	100
Reaction stress [MPa]	0	92.2

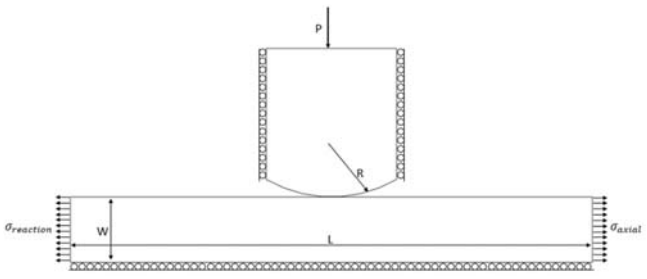

Figure 3 Geometric and loading conditions of fretting contact.

The model is discretized using a 2D quadrilateral, 4-node, plane strain, reduced integration element (CPE4R). For accurate results, the characteristic mesh was selected as 5 μm (Figure 4). The contact between the pad and the specimen was described by utilizing master slave algorithm in ABAQUS [15]. The simulation of contact friction was achieved by using Lagrange Multiplier formulation for the tangential behavior and Augmented Lagrange Algorithm for the normal behavior. Multi-Point Constraint (MPC) was used at the top of the pad in model in order to prevent pad from rotating because of the applied loads. The material of the specimen and pad was selected as Al2024 T3. The modulus of elasticity is 72.1 GPa and the Poisson's ratio is 0.33 for Al2024 T3.

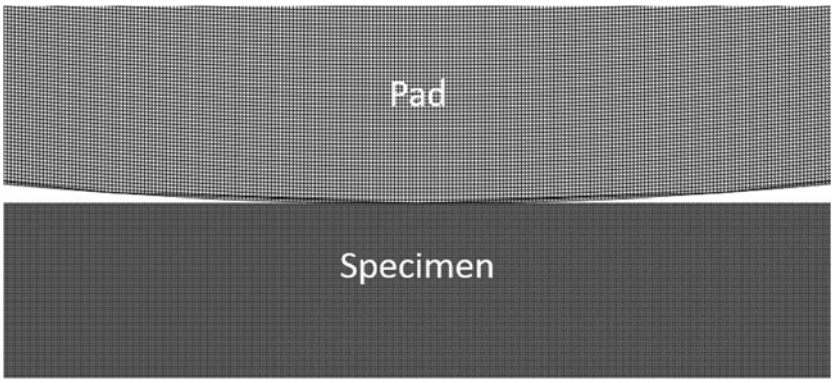

Figure 4. A close-up view of the contact region of the finite element model.

4. Results and Discussion

Materials are not homogeneous and voids may exist in materials. Murakami and Endo [16] reported the effect of these voids in engineering alloys were crucial for fatigue crack formation. To observe the effect of a void, a circular hole was generated under the contact region in the substrate [17]. The position and size of the void was changed, in Figure 5a and 5b, respectively, to investigate the effect on the stresses at the contact surface.

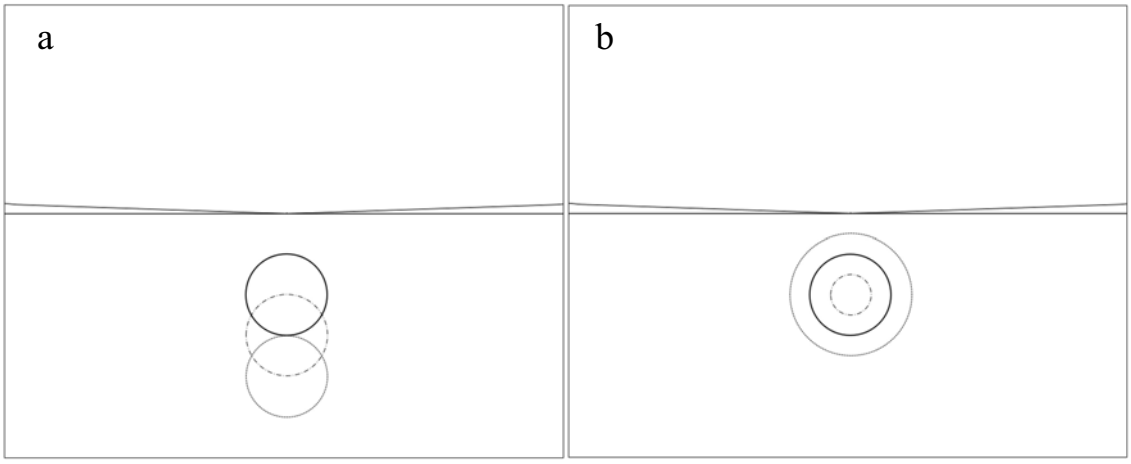

Figure 5. Voids in the substrate (a) at different distance of the centroid from the contacting edge in the finite element model, (b) with different void radius

In the first case, Figure 5a, the distance of the center of circular void to the contact surface is selected as h=0.2, 0.3 and 0.4mm. The von Mises stress distribution for no hole case and hole distance of 0.2, 0.3 and 0.4 are shown figure 6a, 6b, 6c and 6d respectively. It is seen that when the void is closest to the surface, the stresses at the contact region actually increases. However, as the void is moved away by a distance of r or 1.5r, the von Misses stresses at the sliding surface is decreased. It is observed that

hertz contact theory cannot predict the results approximately in terms of contact pressure when voids inserted to the material. The von Mises stress distribution for no hole case and hole distance of 0.2, 0.3 and 0.4 are shown figure 6a, 6b, 6c and 6d respectively.

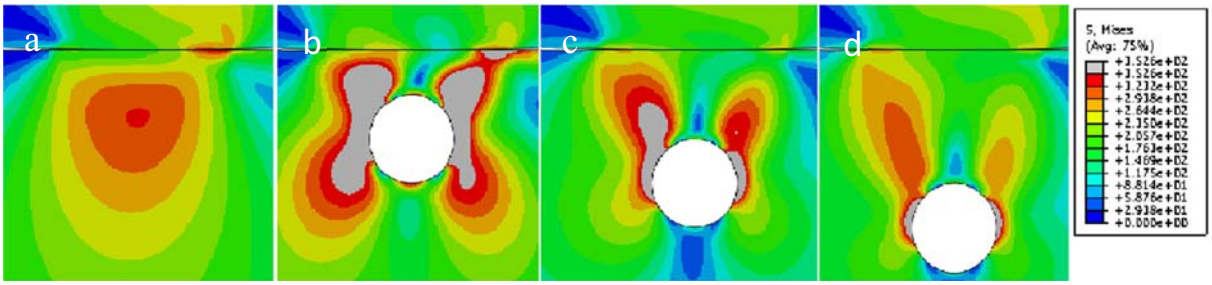

Figure 6. Von Mises stress contours (a) no hole (b) hole distance equal to 0.2 (c) hole distance equal to 0.3 (d) hole distance equal to 0.4

Figure 7 shows the normal traction (Figure 7a) and shear traction (Figure 7b) on the interface, the axial stress in the substrate (Figure 7c) and the relative slip amplitude (Figure 7d) at the contact surface. We will focus on the results for the case when the hole is one radius away from the surface. The peak value of the contact pressure decreases when the void is close to the surface (Figure 7a). The maximum value of the shear traction distribution decreases at the right edge of the contact area while increasing at the left contact region (Figure 7b). The maximum tangential stress tends to increase when the hole becomes closer to the surface. In contrast, the introduction of the void increases the maximum axial stress for the closest void (Figure 7c). Relative slip amplitude decreases when the void is inserted (Figure 7d). Thus, the insertion of a void decreases the frictional shear stresses and relative slip while increasing the normal axial stresses.

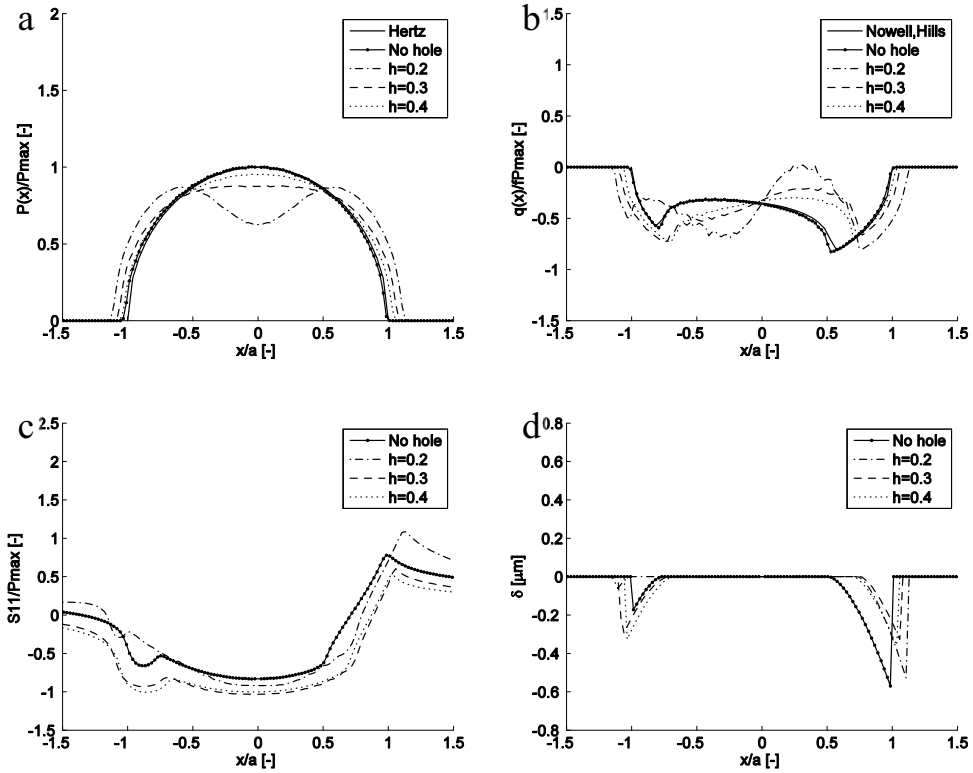

Figure 7. Variation of (a) normalized contact pressure distribution (b) frictional shear stress (c) normalized axial stress (d) relative slip amplitude along the contact surface between the pad and the specimen.

The second comparison is done by the fixing distance between center of void and contact surface and changing its radii which are chosen as 0.05, 0.1 and 0.15mm. The von Mises stress distribution for no hole case and hole radii of 0.05, 0.1 and 0.15mm are shown in figure 8a, 8b, 8c and 8d respectively.

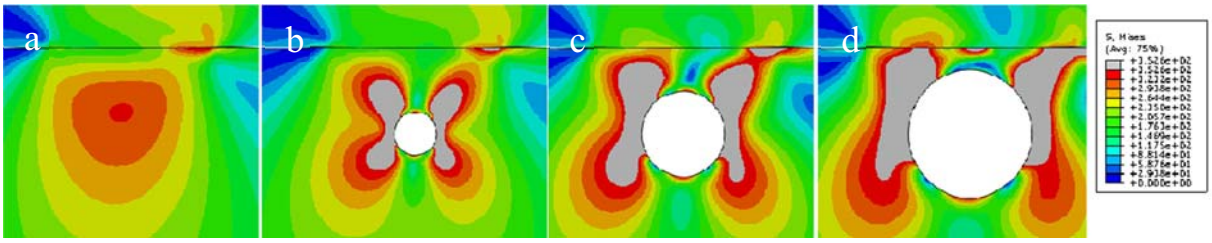

Figure 8. Von Mises stress contours (a) no hole (b) hole radius is equal to 0.05 (c) hole radius is equal to 0.1 (d) hole radius is equal to 0.15

It is seen that contact pressure drops suddenly at the center of the contact region when the void radii increases (Figure 9a). Furthermore, shear traction distribution changes dramatically by changing the void radii (Figure 9b). The maximum value of the tangential stress is also increases (Figure 9c). The stick/slip relation in the contact area depends on both the contact pressure and shear traction distribution. The decreases in the contact pressure at the center of the contact area may leads to slip in this region. When the void radius takes its maximum value relative slip occurs at the center of the contact are (Figure 9d).

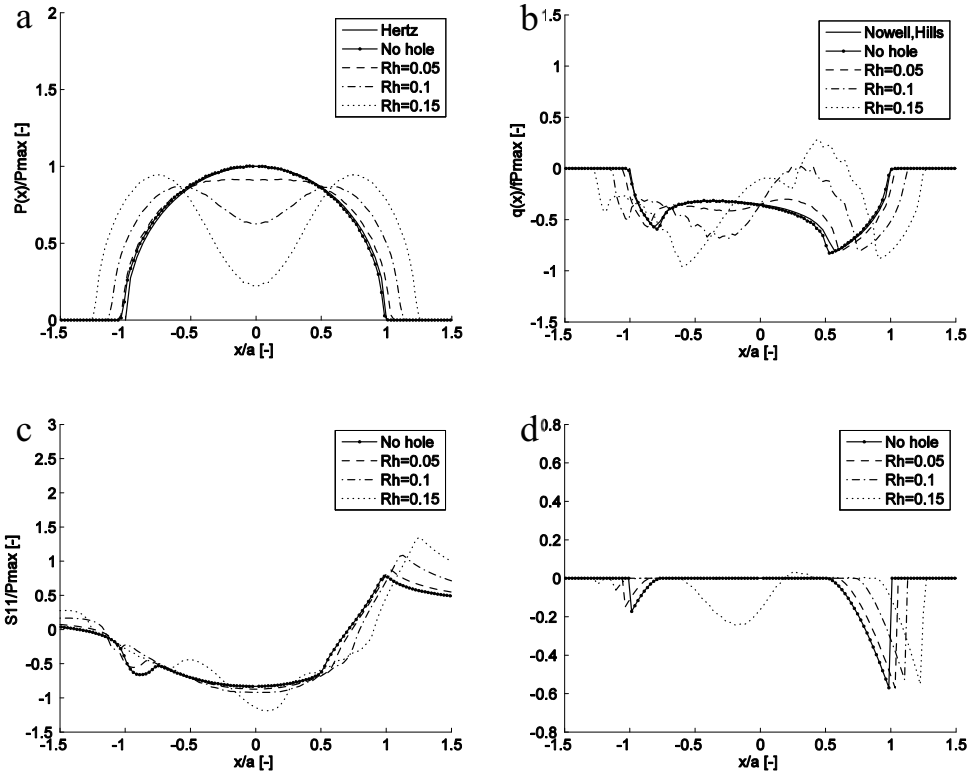

Figure 9. Variation of (a) normalized contact pressure distribution (b) frictional shear stress (c) normalized tangential stress (d) relative slip amplitude along the contact surface between the pad and the specimen.

In the next case, the effect of the multiple voids are considered. An array of 3 by 5 circular voids with radius 0.1 mm is located next to the contact plane in the substrate as shown in Figure 10. The von

Mises stress distribution for no hole case, single hole and multiple holes cases are shown in the figure 11a, 11b, 11c and 11d respectively.

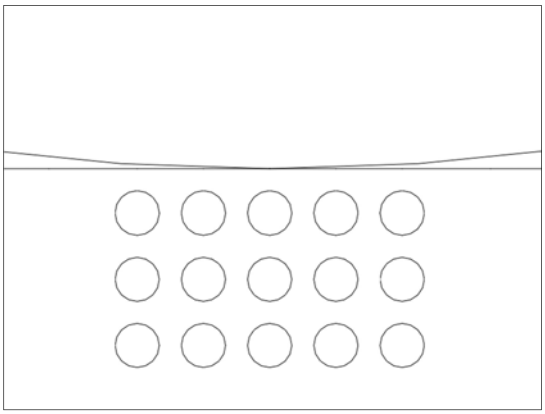

Figure 10. Substrate with an array of voids.

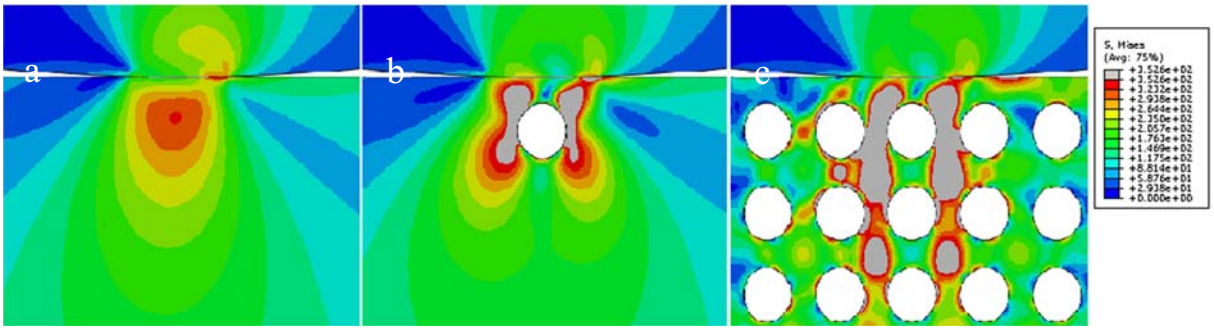

Figure 11. Von Mises stress contours (a) no hole (b) single hole (c) multiple holes

Figures 12a, 12b show that the maximum value of the contact pressure and the shear traction distributions are similar when the single and multi-void results are compared. However, it is seen that contact region increases in the multi-void case (Figure 12a). The effects of the multi voids becomes apparent in terms of maximum tangential stress values and relative slip magnitudes. The maximum value of the tangential stress decreases in the trailing edge of the contact area in the multi voids case (Figure 9c). In contrast, the relative slip amplitude increases (Figure 9d).

5. Conclusions

In this work, fretting contact conditions between a cylindrical pad and a flat specimen are examined for nonhomogeneous materials using finite element analysis. The summary of this work is as follows,

- The effect of the distance between contact region and the center of void is examined. According to the results, both contact pressure and relative slip amplitudes, which is important for the crack nucleation, decreases with increasing the diameter of hole size.

- The maximum value of the tangential stress rises with increasing with hole size. Furthermore, slip takes place at the contact center when these increments are severe.

- The multiple hole case is also examined. The general behaviour of the contact in terms of pressure, shear traction tangential stress distribution are similar for specimens consist of single hole and multiple holes. On the other hand, maximum value of the relative slip amplitudes of the specimen with multiple holes is higher than single hole case.

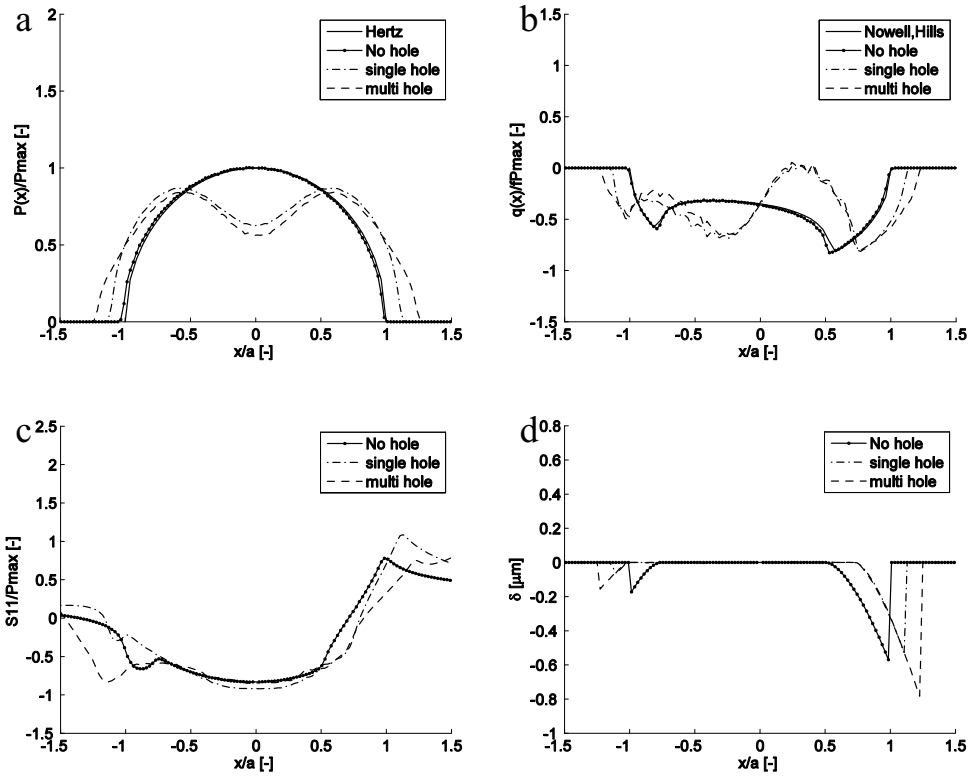

Figure 12. Variation of (a) normalized contact pressure distribution (b) frictional shear stress (c) normalized tangential stress (d) relative slip amplitude along the contact surface between the pad and the specimen.

References

1. Waterhouse, R. B., 1992. Fretting fatigue. The Institute of Materials and ASM International, 77-97.
2. Hertz., H., 1881. On the contact of elastic solids. 156-171.
3. Mindlin, R. and Deresiewica, H., 1953. Elastic spheres in contact under varying oblique forces. Journal of applied mechanics, 20.
4. Nowell, D., and Hills, D. A., 1986. Mechanics of fretting fatigue tests. International Journal of Mechanical Sciences 29(355-365).
5. Nowell, D., 1988. An analysis of fretting fatigue. Thesis (Ph. D.).
6. Ruiz, C., Boddington, P., and Chen, K., 1984. An investigation of fatigue and fretting in a dovetail joint. Experimental Mechanics, 24(3):208 217.
7. Stover, R. J., Mabie, H. H., and Furey, M. J., 1985. A Finite Element Investigation of a Bearing/Cartridge Interface for a Fretting Corrosion Study. Journal of Tribology,107(2), 157.
8. Lee, H., Jin, O., and Mall, S., 2003. Fretting fatigue behavior of Ti-6Al-4V with dissimilar mating materials. International Journal of Fatigue, 393-402.
9. Giner, E., Sukumar, N., Denia, F., & Fuenmayor, F., 2008. Extended finite element method for fretting fatigue crack propagation. International Journal of Solids and Structures, 45(22-23), 5675-5687.
10. Kim, S. H., 2011. Two dimensional and three dimensional finite element analysis of finite contact width on fretting fatigue. Materials Transactions, 147-154.

11. Korkmaz, Y., and Coker, D., 2017. Finite element analysis of fretting contact for dissimilar and nonhomogeneous materials. International Conference of Structural Integrity.
12. Nicholas, T., 2006. High Cycle Fatigue: A Mechanics of Materials Perspective. Elsevier.
13. Hojjati Talemi, R., 2014. Numerical Modelling Techniques for Fretting Fatigue Crack Initiation and Propagation (Unpublished master's thesis). Ghent University.
14. Hojjati-Talemi, R., Wahab, M. A., Pauw, J. D., and Baets, P. D., 2014. Prediction of fretting fatigue crack initiation and propagation lifetime for cylindrical contact configuration. Tribology International, 76, 73-91.
15. ABAQUS (2014) `ABAQUS Documentation', Dassault Systèmes, Providence, RI, USA.
16. Murakami, Y. and Endo, M., 1994. Effects of defects, inclusions and inhomogeneities on fatigue strength. International Journal of Fatigue, 16(3):163–182.
17. Kumar, D., Biswas, R., Hien Poh, L., and Wahab, M. A., 2017. Fretting fatigue stress analysis in heterogeneous material using direct simulations in solid mechanics. Tribology International, 109, 124-132.